

DETERMINATION OF THE TANTALUM-
ZIRCONIUM PHASE DIAGRAM

by

Daniel Eugene Williams

A Thesis Submitted to the
Graduate Faculty in Partial Fulfillment of
The Requirements for the Degree of
MASTER OF SCIENCE

Major Subject: Nuclear Engineering

Approved:

Signatures have been redacted for privacy

Iowa State University
Of Science and Technology
Ames, Iowa

1961

TABLE OF CONTENTS

	Page
INTRODUCTION	1
APPARATUS AND PROCEDURE	4
RESULTS AND DISCUSSION	22
SUMMARY	55
ACKNOWLEDGMENTS	56
BIBLIOGRAPHY	57

INTRODUCTION

The constituent metals of this alloy system have only been used extensively for about the past decade although both have been available for a considerably longer period. The first attempts to isolate zirconium were made by Berzelius in 1824. He employed a potassium reduction of potassium zirconium fluoride but failed to obtain a malleable product. After several intervening attempts with alterations of Berzelius' method by various workers, Lely and Hamburger in 1914 prepared ductile zirconium by the bomb reduction of zirconium tetrafluoride with sodium. With the perfection of the Kroll process for the production and the iodide process for the refinement of zirconium, sufficient quantities of high purity metal were made available for nuclear, chemical, electronic and other applications.

The low thermal neutron capture cross section and the relatively high strength and corrosion resistance of zirconium are properties which enhance its application as a core structural and fuel diluent material in nuclear reactors. Because of its satisfactory corrosion resistance, zirconium is used as a container and structural material in the chemical industry. Zirconium is used as a getter in electronic tubes because of its affinity for oxygen at high temperature. This same property prevents the high temperature application of pure zirconium and many zirconium alloys in other than an

inert atmosphere.

The discovery of tantalum was made by Ekeberg in 1802 but it was not until about 1905 that von Bolton produced relatively pure and ductile tantalum. The early uses of tantalum were as a lamp filament material and as a carbide stabilizing additive in certain types of steel. Some of the more recent applications include chemical containers and process equipment, electrolytic capacitors, vacuum furnaces and crucible material. Tantalum must also be protected from oxidation at elevated temperatures.

The investigation of the tantalum-zirconium system was undertaken as part of a program to obtain information regarding the properties and phase relationships of the alloys of refractory metals with those having application in nuclear reactor technology. Most of the previous work concerning this alloy system consisted of partial phase investigations and the determination of the mechanical properties of the zirconium-rich alloys. Anderson, et al. (1) studied alloys containing up to 30 w/o tantalum as part of an investigation of several zirconium alloy systems. They reported a solubility of about 10 w/o for tantalum in beta zirconium and virtually no solubility in the alpha phase. The beta solid solution was reported to decompose eutectoidally. These investigators also determined some of the mechanical properties of the alloys at room temperature and 650°C.

Pfeil (2) investigated the hardness and microstructure of several alloys and suggested that the system contains no eutectic but that the light phase in the eutectic-like microstructure of the intermediate alloys is an intermediate phase or a tantalum-rich solid solution. Litton (3), Keeler (4), and Chubb (5) conducted separate investigations on zirconium alloys to determine the mechanical properties at ambient and elevated temperatures. Van Thyne and McPherson (6) reported the tensile properties and tentative phase relationships of zirconium-base alloys containing up to 20 w/o tantalum. From metallographic observations they concluded that the beta phase decomposes eutectoidally at a composition of about 10 w/o tantalum and that the maximum solubility of tantalum in alpha zirconium is less than 5 w/o. Emelyanov, et al. (7) studied the tantalum-zirconium system by metallography, thermal analysis, electrical resistance measurements, and X-ray diffraction and concluded that the system is of the eutectic type with limited solubility. The reported values of the eutectic temperature and composition are 1585°C and 50 w/o tantalum respectively. The solubility limits at the eutectic temperature were given as 27 w/o at the zirconium-rich end and 9 w/o at the tantalum-rich end. The beta solid solution is reported to decompose eutectoidally at 790°C and 13 w/o tantalum.

APPARATUS AND PROCEDURE

The Preparation of Alloys

Materials

The zirconium used in the investigation was obtained from the Atomic Power Division of the Westinghouse Electric Corporation. The material is low-hafnium crystal bar zirconium which had been arc melted and fabricated into plates. The tantalum was supplied by the Fansteel Metallurgical Corporation in the form of high purity sheet. The analyses of the materials are given in Table 1.

Melting

Melting was accomplished in a non-consumable, tungsten-electrode arc furnace constructed at the Ames Laboratory and described by Levingston and Williams (8). The alloys were melted under an atmosphere of helium after evacuation of the chamber to a pressure of less than 10^{-5} mm Hg. After admission to the furnace chamber, the helium was purified by melting a charge of zirconium. The water-cooled copper hearth contains molds for making button-shaped and rod-shaped ingots. Both shapes were used in the preparation of the tantalum-zirconium alloys. Charges containing 70 to 80 grams of tantalum and zirconium in appropriate proportions were placed in the molds and melted at least six times. The ingots were inverted after each melting to facilitate mixing

and promote homogeneity. The button-shaped ingots were about 1.5 inches in diameter and 0.5 inch thick. The rod-shaped ingots were approximately 3 inches long and 0.5 inch in diameter. The weight loss due to vaporization and splattering during melting was seldom greater than 0.1 gram which would constitute an uncertainty of about ± 0.15 w/o. All compositions subsequently reported are intended compositions on a weight percentage basis.

Table 1. Analysis of the materials used in alloy preparation^a

Impurity element	Concentration in tantalum, ppm	Concentration in zirconium, ppm
Aluminum	--- b	30
Calcium	Trace	Trace
Carbon ^c	< 100	100
Chromium	--- b	30
Copper	Trace	Trace
Hafnium	--- b	--- b
Hydrogen ^d	0.5	31
Iron	40 ^c	< 200
Magnesium	Trace	Trace
Nickel	---b	20
Nitrogen ^d	2	22
Oxygen ^d	235	85
Titanium	200 ^c	20

^aThe concentrations were determined by spectrographic analysis unless otherwise noted.

^bNot detected in spectrographic analysis.

^cDetermined by analytical chemical methods.

^dDetermined by vacuum fusion analysis.

Fabrication

The ingots were fabricated into specimens by several different means. Simple cutting was carried out with a silicon carbide abrasive saw using water as a coolant. Machining operations such as turning, milling and drilling were successfully performed on all the alloys. The alloys were reduced to wire with diameters as small as 0.030 inch by rotary swaging and further reduction was effected by drawing. Specimens containing less than 5 w/o tantalum could be readily swaged with no special heat treatment. The remainder of the alloys required at least one intermediate annealing step during the swaging operation. Only the intermediate alloys were drawn to diameters smaller than the 0.030 inch obtained by swaging. In order to prevent galling during drawing, an oxide coating was applied by electrolysis in a one per cent sodium sulphate solution and the wire was then lubricated with tallow. The wires were reduced to 0.015 inch diameter by drawing. The alloys were fabricated into sheet with a standard motor-driven rolling mill. A hand operated rolling mill was used for small sheet specimens and for Fed rolling. Hot swaging and hot rolling operations were conducted at 800°C to 900°C with specimens enclosed in air-tight steel jackets which were subsequently removed by machining.

Melting Point Determinations

The melting points of the tantalum-zirconium alloys were determined with the apparatus described by Williams (9) which is based on the method of Pirani and Alterthum (10). This method consists of heating the bar-shaped specimen by its own resistance to an electric current carried by water-cooled copper electrodes and clamps. Heating was carried out in a chamber continuously evacuated to a residual air pressure of less than 10^{-5} mm Hg. Temperature measurements were made with a Leeds and Northrup optical pyrometer through a glass covered observation port in the top of the chamber. The pyrometer was focused on a hole drilled in the specimen to a depth greater than four times the hole diameter. This depth to diameter ratio was shown adequate to produce nearly black-body conditions by checking the melting points for zirconium, niobium, uranium and other metals using holes of this proportion.

The temperature was increased slowly and ample time was allowed for the specimen to attain equilibrium. When the temperature of the specimen just exceeded its solidus temperature, a drop of liquid formed in the bottom of the sight hole. This destroyed the black-body conditions and produced a dark spot in the hole. Temperature measurements were made in the hole and on the surface of the bar immediately adjacent to the hole after equilibrium was attained

following each temperature increase. These measurements provided a relationship between the black-body temperature and the surface or apparent temperature for the alloy being tested. As more liquid formed with rising temperature the hole disappeared and only the surface temperature was measured until the bar melted completely in two. The surface temperature at melting was corrected for emissivity error by an extrapolation of the black-body vs. apparent temperature relationship which was obtained below the solidus. The resulting corrected temperature is only an approximate value of the liquidus for the alloy. Possible sources of error include the fact that the bar may fall apart due to lack of mechanical strength even though some solid material remains. An error of opposite sign would be introduced if the surface tension of the liquid were sufficient to keep the bar intact past the true liquidus temperature. The error due to the extrapolation of the relationship between the apparent and black-body temperatures past the solidus temperature is relatively small for this alloy system since the liquidus and solidus are separated by a small temperature difference over the entire diagram. Despite the uncertainties of this method when applied to liquidus determinations, it was the most practicable one available.

A set of Bausch and Lomb neutral density filters was used to extend the effective limits of the optical pyrometer.

The pyrometer and filters were calibrated with a single filament lamp having a known current-temperature relationship. The calibration curves for the neutral density filters are contained in Figure 1.

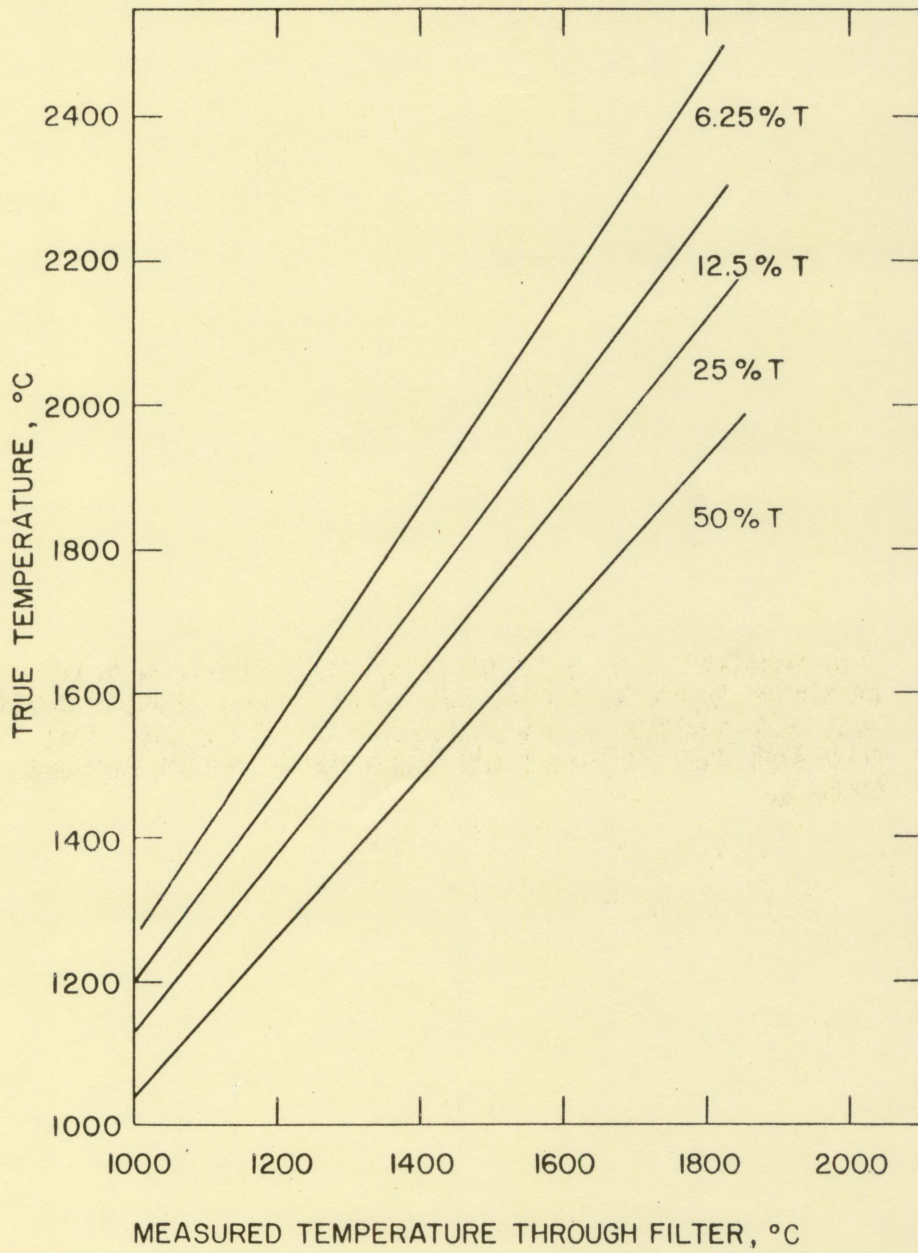
Electrical Resistance Determinations

The variation of electrical resistance of the tantalum-zirconium alloys with temperature was investigated from room temperature to 1800°C. Two different methods were used, one for the range from room temperature to 1000°C and another for the 1000°C to 1800°C range.

In the low temperature range, U-shaped specimens prepared from 0.03 inch diameter wire were heated in a vacuum by a resistance furnace. A pressure of less than 5×10^{-6} mm Hg was maintained throughout the experiment. A direct current of 50 to 100 ma. was passed through the specimen and a standard resistor connected in series outside the furnace. By measuring the drop in potential across each, the current flowing and the resistance of the specimen were determined. Platinum wires spot welded to the specimen were used for the current and potential leads. Temperature measurements were made with a platinum/platinum-rhodium thermocouple welded to one leg of the specimen. A diagram of the electrical circuit is contained in Figure 2.

A potentiometric method was also used in the high temperature resistance experiments but with the following

Figure 1. The calibration curves prepared for a set of neutral density filters. The known temperature vs. the measured temperature with filter are plotted for filters of different transmission value.



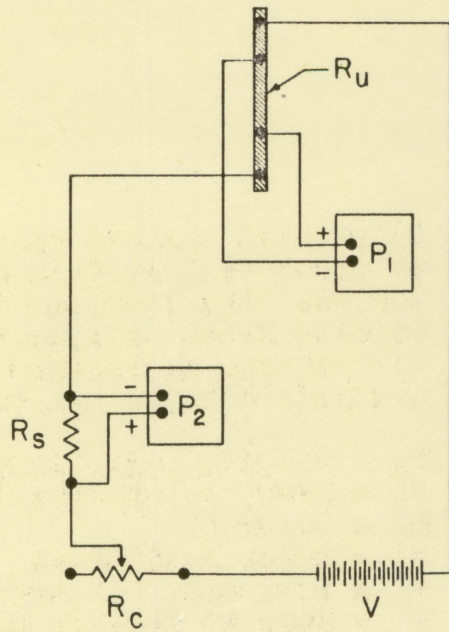
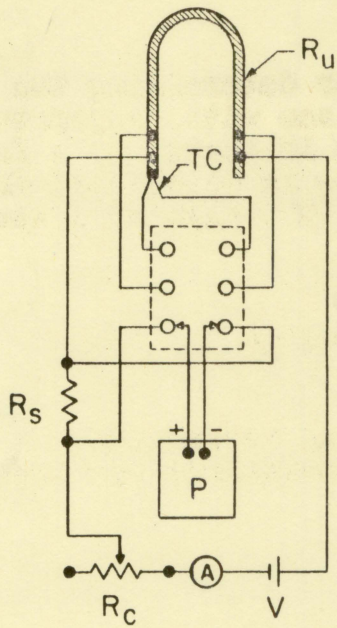
modifications. The specimen was a straight wire and was heated by its resistance to a large direct current. The specimen was supported by water-cooled copper electrodes inside a chamber evacuated to less than 10^{-5} mm Hg. The potential drops along a portion of the wire and across an external series resistor were measured. From these data the resistance of the specimen was calculated. Since temperatures approaching the melting point of platinum were attained in these experiments, 0.01 inch diameter tantalum wire was used to measure the potential drop along the specimen. The temperature of the specimen was measured with an optical pyrometer. Since the diameter of the specimen was too small to permit drilling a sight hole, the relationship between black-body and apparent temperature determined for the alloys in the solidus investigation was used to correct the observed temperature measurements. This method of temperature measurement was shown to be satisfactory by using it to check the melting points of some of the alloys. The heating current was supplied by a group of storage batteries and was varied with a series of load resistors constructed of Nichrome strip. The electrical circuit for this apparatus is included in Figure 3. The object of the resistance temperature measurements was to locate the phase transformations of the alloys by observing the anomalies in their resistance curves. No attempt was made to obtain the absolute resistivity of the

Figure 2. Electrical circuit for determining the variation of electrical resistance with temperatures up to 1200°C. The specimen is heated by a furnace and the unknown resistance is calculated from the potential drop due to the flow of a small direct current.

A - D C milliammeter
P - Rubicon potentiometer
 R_u - Specimen
 R_s - Known resistance
 R_c - Current regulating resistance
TC - Platinum/platinum-rhodium thermocouple
V - Storage cell

Figure 3. Electrical circuit for determining the variation of electrical resistance with temperatures above 1000°C. The specimen is heated by a large direct current which is also the current used to calculate the unknown resistance. Temperature measurements are made with an optical pyrometer.

P_1 - Rubicon potentiometer
 P_2 - Brown potentiometer
 R_u - Specimen
 R_s - Known resistance
 R_c - Load rack for regulating current
V - Bank of storage cells



alloys at elevated temperature.

Dilatometry

Zirconium undergoes a contraction on heating when transforming from the hexagonal to the body-centered-cubic phase. The contraction produces a sharp break in the thermal expansion curve at the transformation temperature. The equipment described by Dooley and Atkins (11) was used to measure the thermal expansion in this investigation. The movable core of a linear variable differential transformer is attached to one end of a fused silica rod the other end of which rests on the specimen. Any change in the length of the specimen is translated into an electric signal by the movement of the transformer core. The amplified output of the transformer is plotted along the Y-axis of a Brown X-Y recorder. Temperature measurements were made with a Chromel-Alumel thermocouple attached to the specimen. The signal from the thermocouple was applied directly to the X-axis of the recorder. The equipment was frequently calibrated using the known transformation temperatures of metals such as iron, zirconium and uranium. The maximum error of the dilatometer was found to be less than 10°C, which includes the error in temperature measurement and any error due to the inability to record or observe the first stages of the inflection in the dilation curve.

The apparatus described above employs a 2000 cps linear

transformer mounted inside the vacuum system. This type of arrangement requires the extension of electrical and mechanical connections through the vacuum chamber. A Wien bridge oscillator was used to supply the primary current for the linear transformer.

A dilatometer was constructed by the author which also used a linear transformer to sense the thermal expansion but with the following modifications. A 60 cps transformer instead of a 2000 cps transformer is used thus eliminating the need for an oscillator. Regulated line voltage is passed through a series of dropping resistors and fed directly to the primary winding of the transformer. By varying this resistance the input voltage can be varied from 2 to 10 volts. The size of the 60 cps transformer is such that it may be mounted outside the vacuum system. The iron core is within the system attached to one end of a fused silica rod as in the Dooley-Atkins apparatus. The secondary voltage of the 60 cps transformer is rectified with a germanium diode and is applied to the Y-axis of the X-Y recorder. The specimen temperature is measured with a platinum/platinum-rhodium thermocouple and is plotted as before on the X-axis of the recorder. This dilatometric apparatus is simpler in construction and operation. All electronic components have been eliminated except standard recording and temperature controlling equipment. The mechanical adjustment of the

position of the transformer winding is readily made by means of a micrometer screw. Complete shielding and grounding of all components in the 60 cps dilatometer is required to prevent the interference of spurious signals from neighboring equipment.

Beck program controlling equipment was used to produce heating and cooling rates as low as about 5°C per hour. The upper limit of the heating and cooling rates was fixed by the characteristics of the furnace since the controlling equipment could be set so that the current remained on or off continuously.

The specimen-supporting tube and the rod connecting the transformer to the specimen were made of fused silica and were so arranged that any error due to expansion of one would tend to be compensated for by the similar expansion of the other. The operating temperature range of the equipment was such that there were no crystallographic inversions in the fused silica members. Both dilatometers were connected to vacuum systems which maintained the pressure within the system below 5×10^{-6} mm Hg during the experiments.

X-Ray Diffraction

All X-ray analyses were performed with filtered copper K α radiation from a General Electric XRD-4 generator. Powder data were obtained with a Phillips diffractometer and with Debye-Scherrer cameras. Powder specimens were prepared by

filing followed by magnetic removal of any iron contamination from the file and then by stress-relief annealing. The specimens were prepared from minus 200 mesh particles. Sheet or small pieces of ingots were suitable for study with the diffractometer. Solid specimens for use in the powder cameras were prepared from wire having a diameter of about 0.015 inch.

All heat treatment of the specimens was done in a vacuum of at least 10^{-5} mm Hg. The powders and small solid specimens were placed in tantalum vessels or wrapped in tantalum foil to prevent reaction with the furnace tubes. Cooling rates following heat treatment were varied by controlled reduction of the furnace current, complete removal of the sample container from the furnace, or by the simultaneous removal of the container and admission of helium to the chamber. Massive specimens were effectively quenched in helium or water.

The techniques employed in the X-ray diffraction studies were consistent with the accepted practices for promoting accuracy. Eccentricity errors were minimized by carefully mounting the specimen along the cylinder axis of the camera. Camera radius and film shrinkage errors were eliminated by employing the Straumanis film mounting technique. To minimize the effect of systematic errors, the lattice parameters were determined from graphical extrapolations of back-reflection data vs. $\cos^2\theta$ or the Nelson-Riley function, $\frac{1}{2}(\sin^2\theta + \frac{\cos^2\theta}{\theta})$. According to Azaroff and Buerger (12) the theoretical accuracy

for the determination of lattice parameters by the powder method is approximately 1 part in 10,000. From a consideration of the methods employed, the accuracy of the lattice parameters obtained in this investigation is about 1 part in 3000.

Metallography

Several features of the diagram were determined or confirmed by metallographic techniques. The metallographic preparation of the tantalum-zirconium alloys was in general difficult and although many variations were tried, only the most successful method will be described. The specimens were ground on 320, 400, 500, and 600 grit silicon carbide abrasive papers with water as a lubricant and coolant. Intermediate polishing was done with 15 micron alumina on a Buehler Microcloth lap. The final polish was effected with 0.3 micron alpha-alumina on Microcloth. The best results were obtained when the alumina abrasive was applied in the form of a paste with water. A chemical polish was developed which was most applicable to zirconium and zirconium-rich alloys. This consisted of polishing as usual to the final stages then polishing with alpha-alumina and a solution of ammonium bifluoride and acetic acid on Microcloth. The strength of the solution was adjusted by varying the amount of water applied to the lap. Electropolishing techniques were also used in the preparation of some of the specimens, particularly those quenched from a solid solution region. A methanol,

ethylene glycol, perchloric acid electrolyte was found to be satisfactory. No further etching was required after electro-polishing or chemical polishing. For alloys polished by ordinary mechanical means, the most satisfactory etchant was a 3:1 mixture of nitric and hydrofluoric acids diluted with water to various strengths depending on the composition and thermal history of the specimen. A cathodic etching apparatus described by Carlson, *et al.* (13) also found limited application in the metallographic preparation of the alloys.

Automatic furnace-controlling and temperature-recording equipment was used in producing the necessary heat treatment of the alloys. The metallographic specimens were quenched by one of the following methods depending on the specimen form and the quenching temperature desired. In the capsule quenching method, small pieces of the ingots or rolled sheet were wrapped in tantalum foil then sealed in evacuated silica capsules. After heating, the encapsulated specimens were quenched by simultaneously dropping and crushing the capsule in a bath of cold water. The method was limited by the properties of silica and the operating limits of the furnace to a maximum temperature of approximately 1200°C. In a second method using water as a quenchant, very small specimens were heated in a tantalum bucket suspended in a vertical quartz furnace tube. After the desired heat treatment, water was admitted by breaking a thin glass plate which formed the

bottom of a vessel at the top of the furnace tube. The water was drawn rapidly into the previously evacuated furnace tube. As the quench was made the furnace was lowered from the tube and swung aside thereby removing the heat source. Several specimens could be quenched at one time and at moderately rapid rates. However, the maximum temperature of operation was approximately 1000°C due to the limitations of the furnace and because of the violent boiling at this and higher temperatures. The most rapid cooling rates were obtained by quenching small diameter wires with helium. The wires were heated by their resistance to an electric current in the apparatus used for high temperature resistance measurements and which has been previously described. The specimens were quenched by simultaneously turning off the electric current and admitting helium to the chamber. Some alloys were quenched from as high as 2200°C but the majority of the quenches were made in the range from 1200°C to 1800°C. Very high cooling rates were obtainable with this method. While no actual measurements of these rates were made, total cooling times of approximately 3 seconds from 1800°C to black-heat were routinely observed. The quenching rate could be varied by changing the diameter of the specimen. The average specimen diameter used in this investigation was approximately 0.030 inch.

RESULTS AND DISCUSSION

The Phase Diagram

The phase diagram constructed from the data obtained in this investigation is presented in Figure 4. The discussion of these data will be presented as they apply to the several significant areas and features of the diagram.

The solidus

The specimens used in the melting point determinations were machined from slabs of the as-cast ingots. Equilibration of the specimens was accomplished during the experiment by heating slowly and annealing for about 2 hours at temperatures just below the melting point. Metallographic examination of specimens after the melting point determination showed that equilibrium had been attained. In general, two specimens were prepared at each composition examined. If the observed melting points did not agree within experimental error, the experiment was repeated. The results of the melting point determinations are summarized in Table 2. The values reported for most of the alloys are the averages of several determinations.

The solidus decreases slightly from the melting point of zirconium and passes through a minimum at 1620°C near 25 w/o tantalum. However, the flatness of the curve in this region prevented the exact location of the minimum point. The

Figure 4. The phase diagram of the tantalum-zirconium system.

- △ - Liquidus points
- ▲ - Solidus points
- - Electrical resistance data
- - Dilatometric data
- ▣ - Coincident electrical resistance and dilatometric data

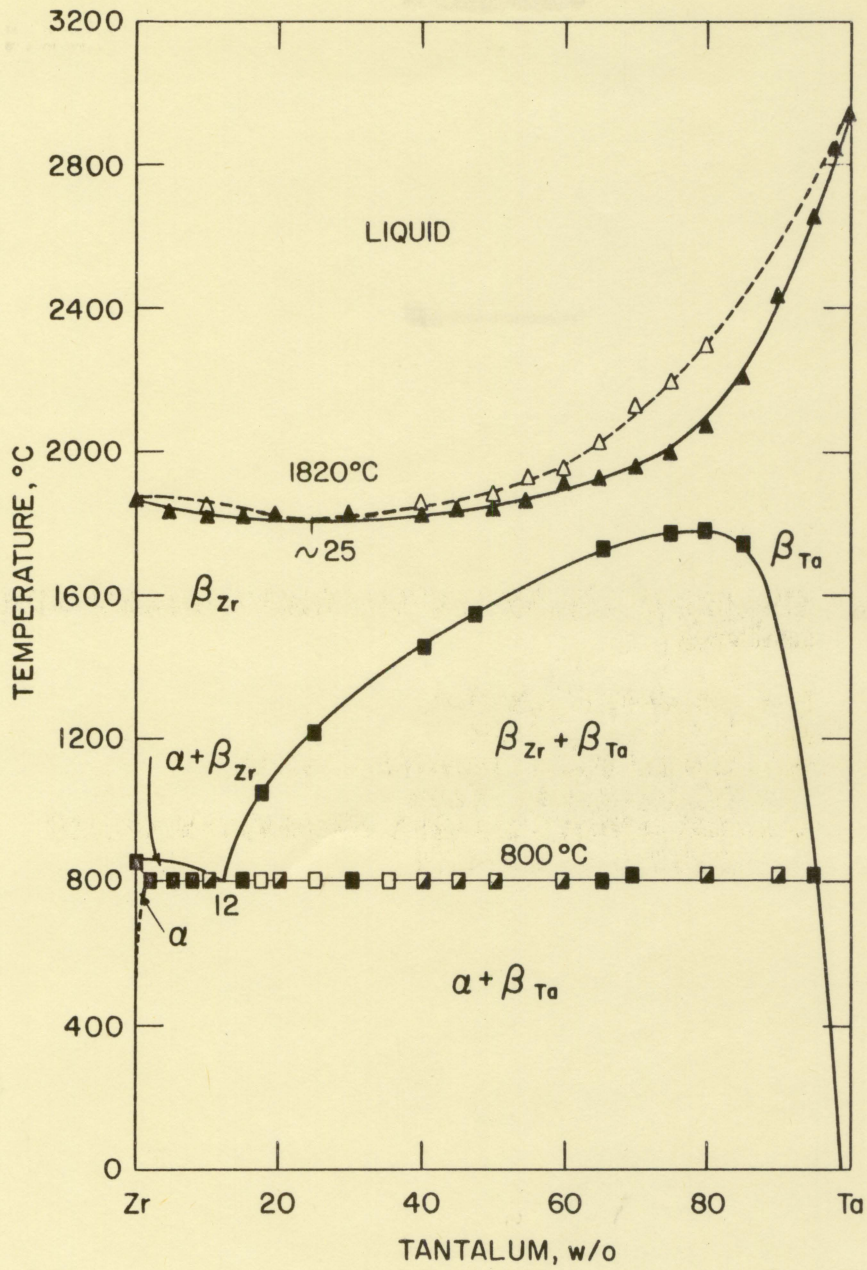


Table 2. Melting points of the tantalum-zirconium alloys

Composition w/o Ta	Melt number	Solidus °C ^a	Liquidus °C ^b
100 w/o Zr	1047	1860	-----
0.25	1110	1858	-----
0.50	1108	1843	-----
0.75	1109	1852	-----
1.00	1106	1846	-----
1.00	1107	1840	-----
1.25	1123	1839	-----
1.50	1124	1836	-----
2.00	1058	1833	1865
3.00	1059	1832	1841
5.00	1060	1827	-----
7.00	1061	1837	-----
10.0	1062	1830	1837
15.0	1063	1822	-----
17.5	1064	1838	1860
20.0	1065	1827	-----
30.0	1066	1830	1848
40.0	1067	1833	1847
45.0	1068	1835	1848
50.0	1069	1841	1870
50.0	1323	1840	-----
55.0	1070	1862	1927
60.0	1071	1907	1939
65.0	1121	1922	2030
70.0	1073	1955	2128
70.0	1046	1953	-----
75.0	1114	1993	2195
80.0	1074	2065	2295
80.0	1047	2065	-----
85.0	1129	2203	-----
90.0	1075	2433	-----
95.0	1076	2653	-----
98.0	1077	2839	-----
100.0	1241	2940	-----

^aThe solidus values reported are averages of at least three determinations.

^bThe liquidus values are considered only approximate.

solidus then rises slowly until a composition of about 50 w/o tantalum is reached after which a more rapid increase is observed. Relatively little separation occurs between the solidus and the liquidus curves over the entire diagram. A maximum difference of about 200°C was observed at 80 w/o tantalum.

In establishing the uncertainty value for the solidus data the following sources of error were considered: the precision of the optical pyrometer, the uncertainty of the method, and the random errors of judgment. It was demonstrated experimentally that the melting point of pure zirconium could be observed within $\pm 10^\circ\text{C}$ of the accepted value using the described method. The instrument and judgment errors were found to be about $\pm 5^\circ\text{C}$ from the results of measurements of the filament temperature of a standard lamp. Thus, for alloys in which a relatively large amount of liquid is produced by a small temperature increment above the solidus, which would include alloys up to about 60 w/o tantalum, the total uncertainty in the melting point determination is about $\pm 15^\circ\text{C}$. The uncertainty is larger for alloys with tantalum content greater than about 60 w/o because the amount of liquid produced by a given temperature increment is smaller than in the lower tantalum alloys. Also, since the melting points of the alloys begin to increase rapidly above 60 w/o tantalum, the higher range of

the optical pyrometer must be employed which decreases the precision of the instrument. Thus, for the range above 60 w/o the limit of accuracy of the solidus is about $\pm 25^{\circ}\text{C}$.

The beta region

Above 860°C zirconium exists in the beta or body-centered cubic modification and according to Eastman and Kerse (14) has a lattice constant of 3.617 \AA and an interatomic distance of 3.132 \AA . Tantalum is a body-centered-cubic metal throughout the entire solid state. Miller (15) gives a lattice parameter value of 3.303 \AA and an interatomic distance of 2.860 \AA at room temperature. The calculated values at 860°C are 3.322 \AA and 2.876 \AA respectively. The atomic diameters of tantalum and beta zirconium differ by about 8.5 percent and therefore have a size factor favoring extensive solid solubility. Considering the size factors, the solubility parameters, and the relative electronegativities, Miller (15) predicts that tantalum-zirconium alloys will show liquid miscibility, extensive solid solubility and little tendency toward stable compound formation.

In this investigation, solid solubility of tantalum in beta zirconium was found to exist across the entire diagram at temperatures just below the solidus. The existence of this phase was indicated by the shape of the solidus and substantiated by metallographic investigation. Photomicrographs of some of the alloys quenched from the beta region

are contained in Figures 5 through 10. The beta modification of unalloyed zirconium could not be retained by any of the quenching methods used in this investigation. However, the beta solid solution of alloys containing more than about 20 w/o tantalum was retained by helium quenching.

The monotectoid loop

Temperature-resistance, X-ray diffraction and metallographic investigations revealed the presence of solid immiscibility in the beta region.

The temperature-resistance curves are plotted in Figure 11. They consist of two linear segments with a slight but reproducible inflection point which was taken to be the temperature of the boundary of the immiscibility region.

X-ray diffraction patterns from a series of samples quenched from 1300°C and 1500°C showed two body-centered-cubic structures having different and constant lattice parameters over a wide composition range, thus revealing the existence of a two phase region extending from approximately 40 w/o tantalum to 85 w/o tantalum at 1300°C and from 55 w/o tantalum to 85 w/o tantalum at 1500°C. The data obtained from these samples are shown in Table 3. By plotting the lattice parameters as shown in Figure 12, the tantalum-rich boundary of the monotectoid loop was established as 93 w/o tantalum at 1300°C and 87 w/o tantalum at 1500°C. A similar procedure could not be followed to determine the zirconium-rich

Figure 5. 20 w/o tantalum
quenched from
1700°C. 250X.

Figure 6. 30 w/o tantalum
quenched from
1700°C. 250X.

Figure 7. 40 w/o tantalum
quenched from
1700°C. 250X.

Figure 8. 50 w/o tantalum
quenched from
1700°C. 250X.

The above photomicrographs illustrate the beta solid solution and are typical of the alloys quenched from that region. All specimens were electropolished and etched with an ethanol-ethyleneglycol-perchloric acid solution.

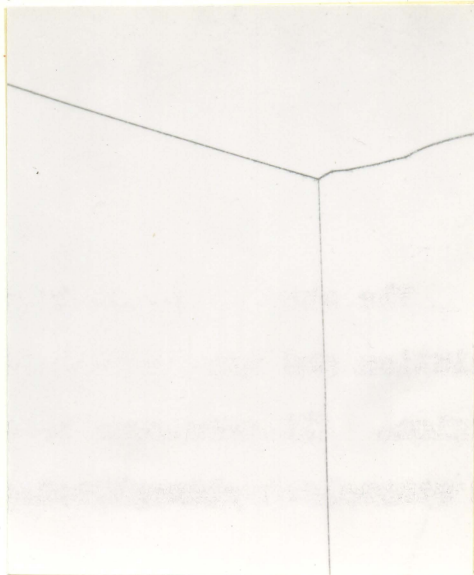
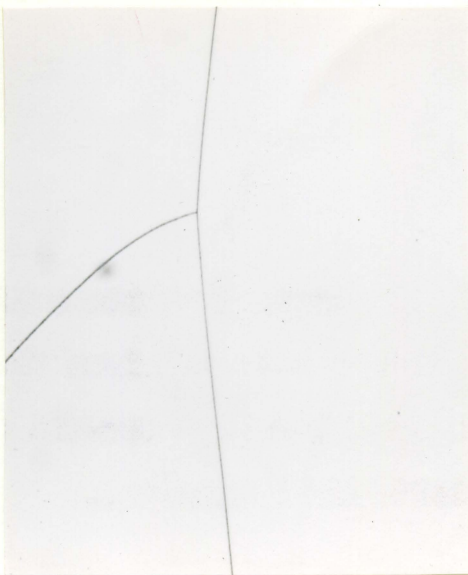
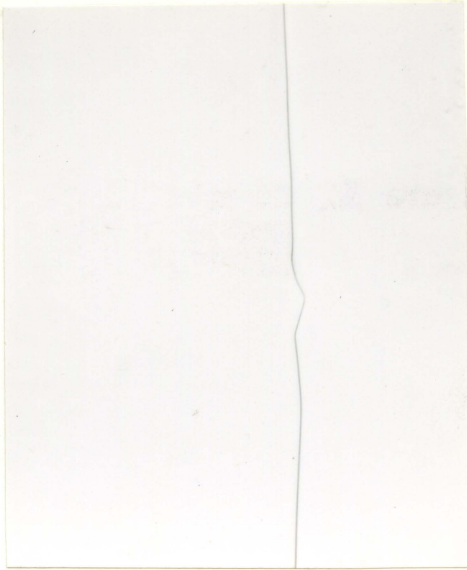
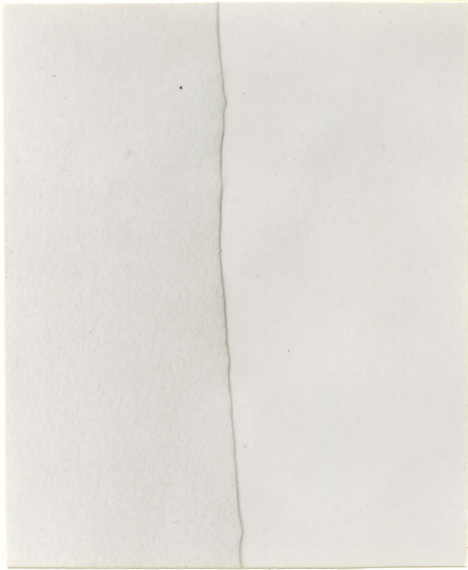
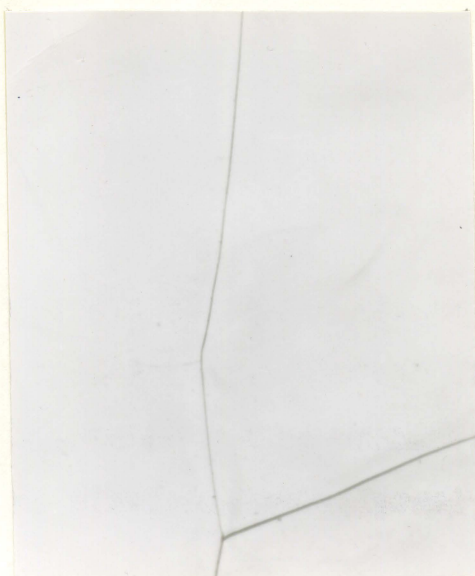
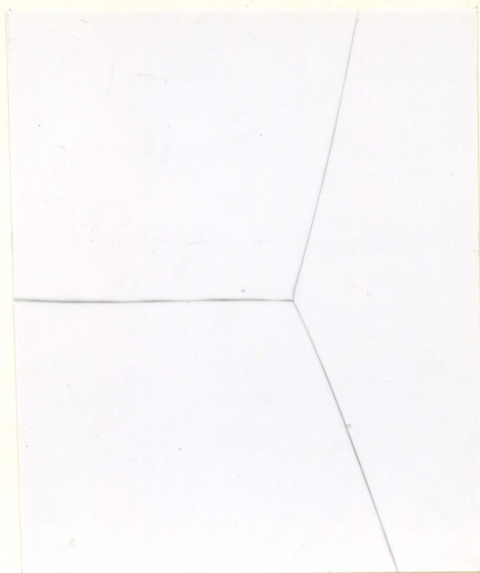


Figure 9. 60 w/o tantalum quenched from 1800°C. 250X.

Figure 10. 80 w/o tantalum quenched from 1900°C. 250X.

The above photomicrographs illustrate the beta solid solution and are typical of the alloys quenched from that region. All specimens were electropolished and etched with an ethanol-ethyleneglycol-perchloric acid solution.






Figure 11. The variation of electrical resistance with increasing temperature of some tantalum-zirconium alloys. The inflection in each curve is indicative of the boundary of the monotectoid loop at that particular composition.

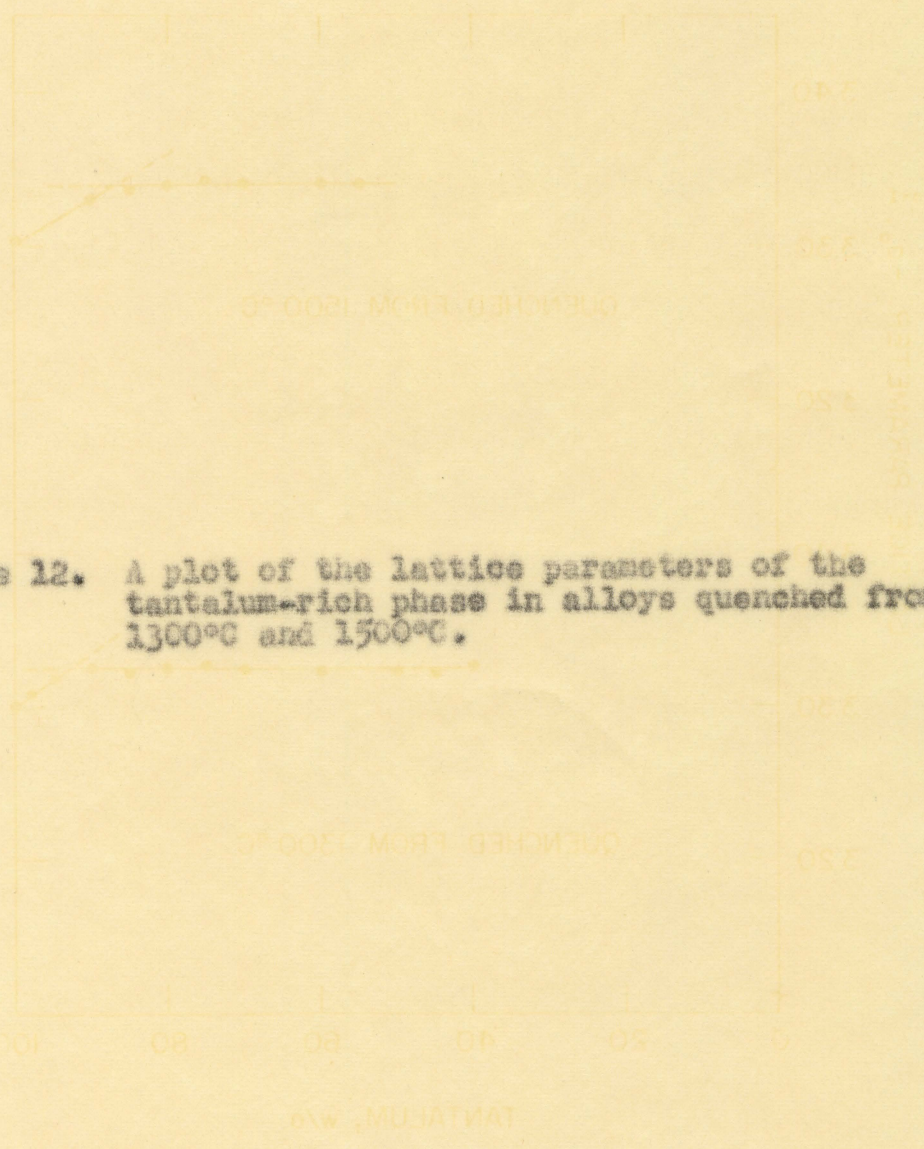


Figure 12. A plot of the lattice parameters of the tantalum-rich phase in alloys quenched from 1300°C and 1500°C.

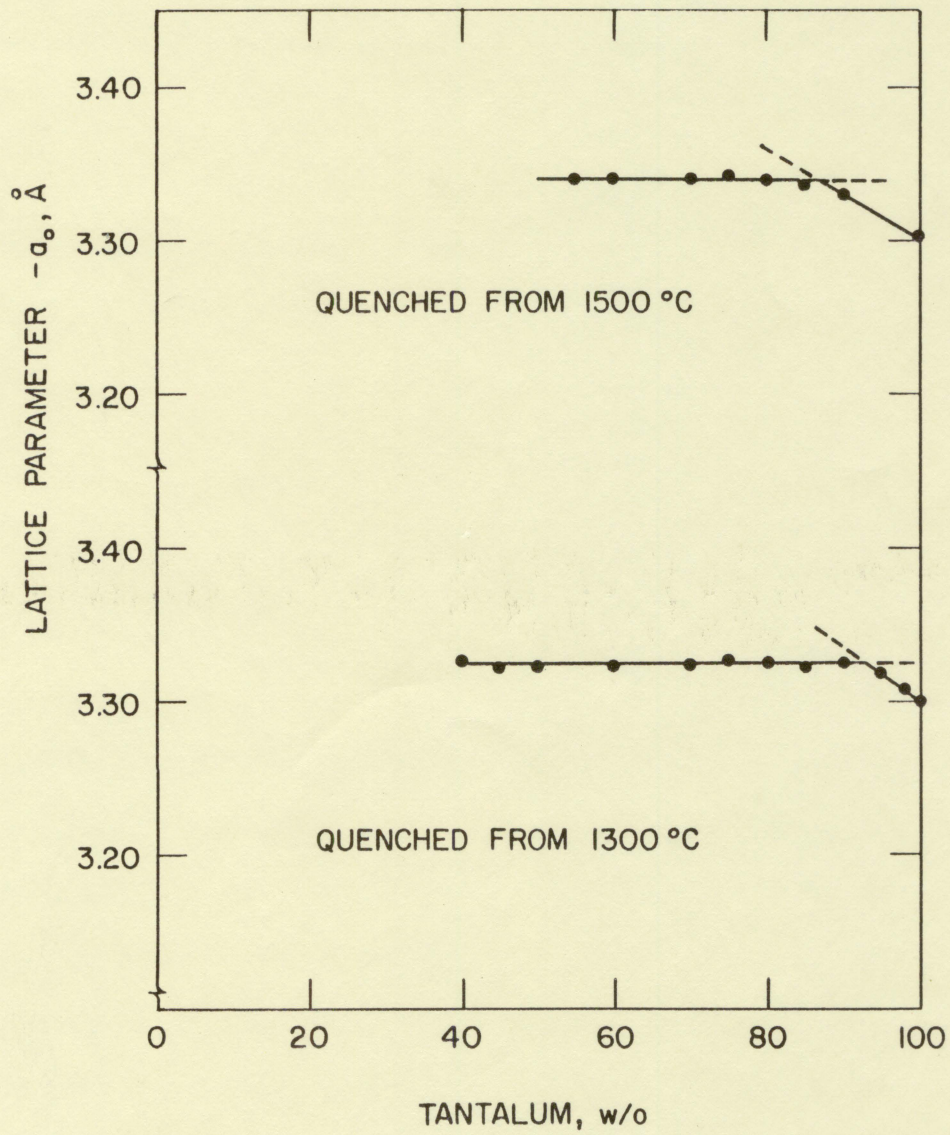


Table 3. Lattice parameter data from quenched alloys

Composition w/o Ta	a_0 , Å-quenched from 1300°C		a_0 , Å-quenched from 1500°C	
	β -Zr	β -Ta	β -Zr	β -Ta
30.0	3.536	-----		
40.0	3.545	3.325		
45.0	3.532	3.323		
50.0	3.544	3.322		
55.0			3.510	3.339
60.0	3.547	3.323	3.514	3.339
70.0	3.545	3.323	3.514	3.339
75.0	3.547	3.326	3.513	3.342
80.0	3.545	3.324	3.51	3.340
85.0	3.5	3.322	present	3.336
90.0	-----	3.325	-----	3.330
95.0	-----	3.318		
96.0	-----	3.307		

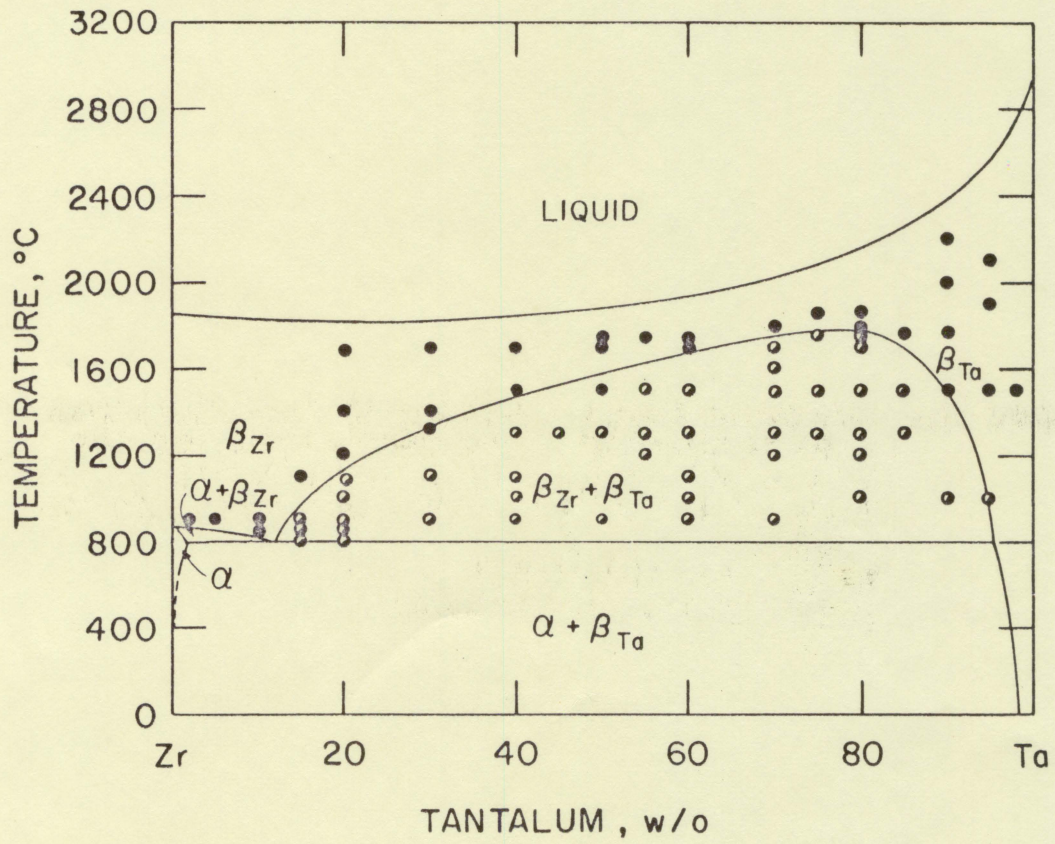
boundary because it was not possible to retain beta zirconium upon quenching.

Metallographic specimens were prepared from alloys of a number of compositions quenched from several temperatures in the vicinity of the monotectoid loop. The number of phases present in these specimens was determined by microscopic examination and the results of this examination are presented graphically in Figure 13. The boundary of the monotectoid loop determined by temperature-resistance and X-ray methods is also shown in Figure 13 and is entirely consistent with metallographic evidence.

The location of the zirconium-rich boundary of the

Figure 13. The phase diagram showing the metallographic data pertaining to the beta region and the monotectoid loop. An enlarged drawing of the monotectoid region is included in Figure 20.

- - Beta solid solution
- - Beta-Ta plus beta-Er



monotectoid loop was determined from resistance-temperature data while the tantalum-rich boundary was located by X-ray diffraction results. The metallographic data confirms the location established by these methods. On the basis of these results, the monotectoid loop is believed to exist from 12 w/o to 95 w/o tantalum at 800°C and reaches a maximum at 80 w/o and 1780°C.

The monotectoid point and the monotectoid isotherm

The beta solid solution decomposes monotectoidally. The nature and details of this reaction were established by electrical resistance, dilatometric and metallographic studies.

Resistance-temperature measurements were used to locate the temperature and the extent of the monotectoid horizontal. A sharp decrease is observed in the resistance of zirconium as the metal transforms from alpha to beta at 860°C. On continued heating through the beta state the resistance again increases. Although the transformation is rapid for pure zirconium, Lustman and Kerze (14) state that a small amount of dissolved oxygen retards the completion of the transformation and the resistance of slightly contaminated crystal bar zirconium which has transformed to beta on heating may not again increase with temperature until a temperature of 900°C or more is attained. From resistance-temperature curves of the alloys, such as those shown in Figure 14, the monotectoid isotherm was found to exist at 800°C and to extend from 2 w/o

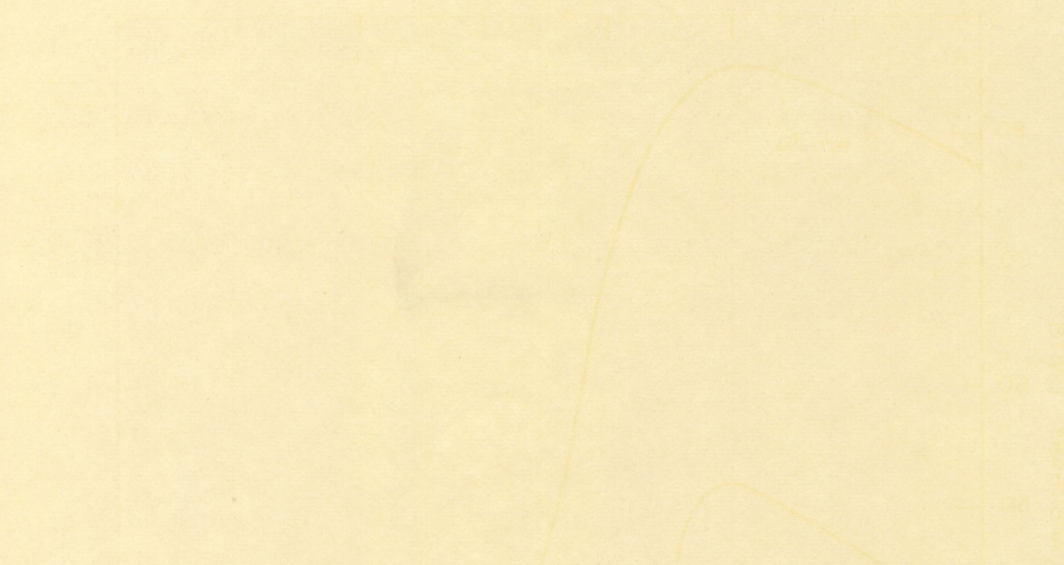
to 95 w/o tantalum. Inflections in length vs. temperature curves such as those plotted in Figure 15 confirmed the temperature of the monotectoid isotherm determined by resistance measurements and also gave points on the upper boundary line of the alpha phase. The complete results of the temperature-resistance and dilatometric experiments are contained in Table 4.

A metallographic study of quenched specimens provided the information for the location of the monotectoid composition and the upper boundary of the alpha plus beta region. Samples were quenched from above the monotectoid and examined for the presence of decomposed beta solid solution and other phases. Figure 16 is representative of a transformed beta structure, while Figures 17 and 18 show the alpha and alpha plus beta structures respectively. Figure 19 shows the appearance of the beta solid solution monotectoidally decomposed. The complete results of the metallographic investigation are plotted as points in Figure 20.

The solubility limits

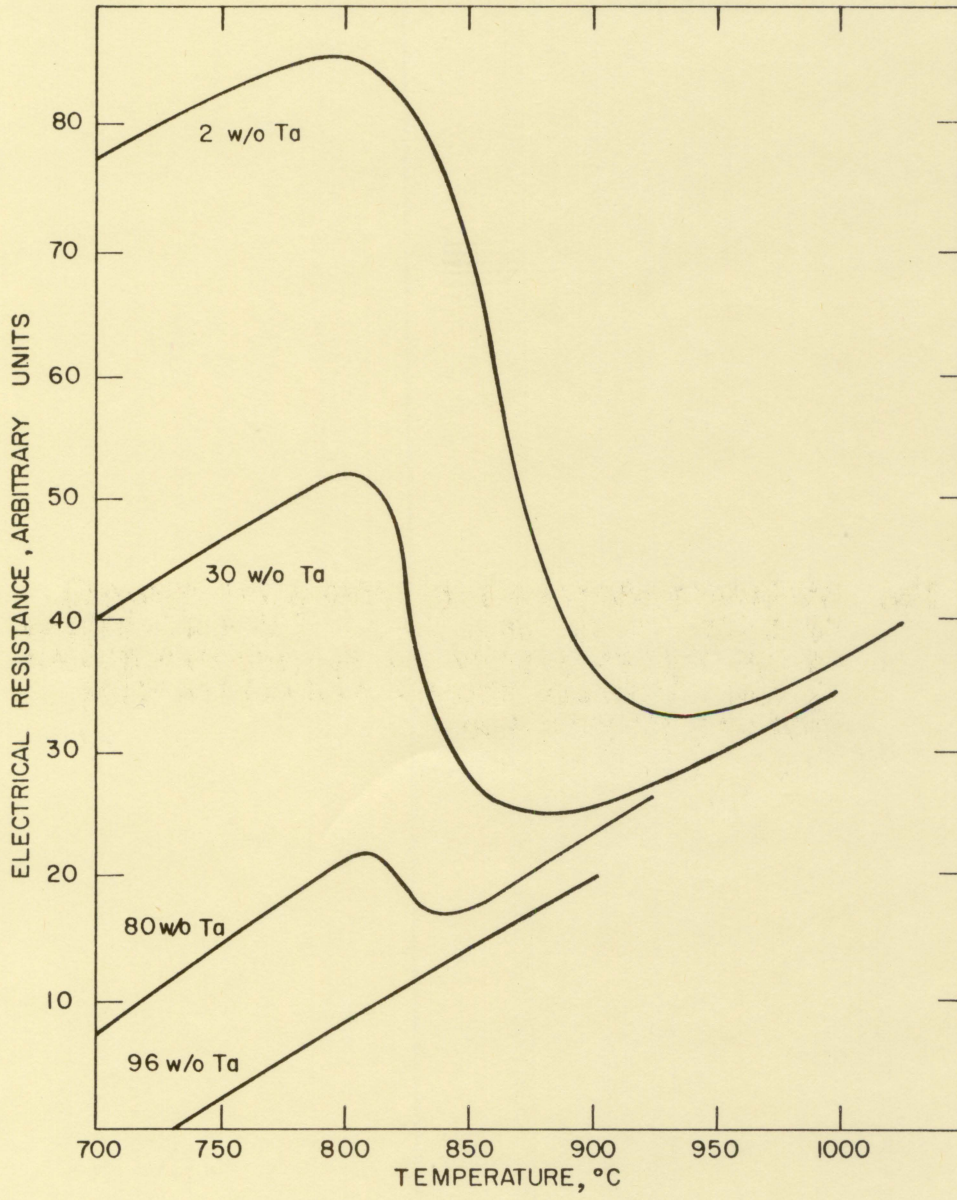
The beta solid solution region has been discussed previously and will not be considered in this section.

Based on temperature-resistance data, Table 4, and metallographic data, Figure 20, the solubility of tantalum in alpha zirconium was established as being slightly less than 2 w/o at 800°C and on the basis of metallographic



The figure shows a graph with a grid. The vertical axis is labeled 'RESISTANCE' and has tick marks at 0, 10, 20, 30, 40, 50, 60, 70, 80, 90, and 100. The horizontal axis is labeled 'TEMPERATURE' and has tick marks at 0, 100, 200, 300, 400, 500, 600, 700, 800, 900, and 1000. There are several curves plotted, each showing a characteristic inflection point. The curves generally show an increase in resistance with temperature, followed by a sharp decrease (inflection) at a specific temperature, and then a further increase. The inflection points occur at approximately 150, 250, 350, 450, and 550 degrees Celsius. The curves are labeled with numbers 1 through 5, corresponding to different alloys.

Figure 14. Resistance-temperature curves for several tantalum-zirconium alloys. The inflections in the curves are due to the transformation of the zirconium phase. All curves were obtained on heating.



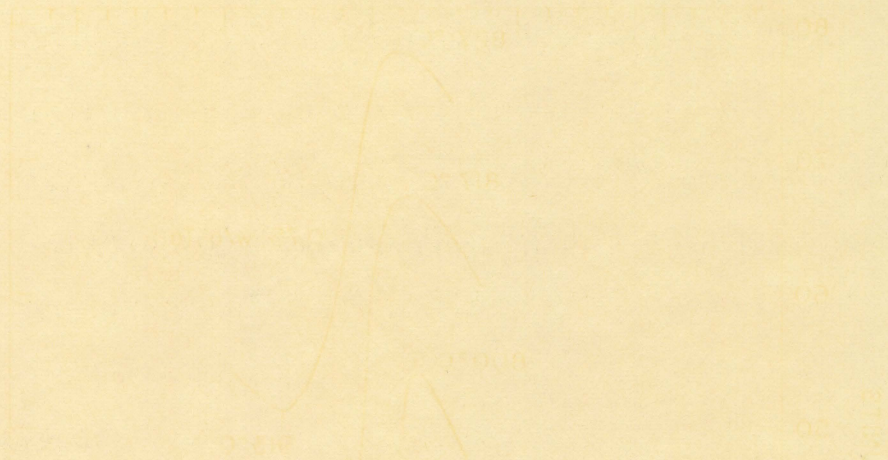
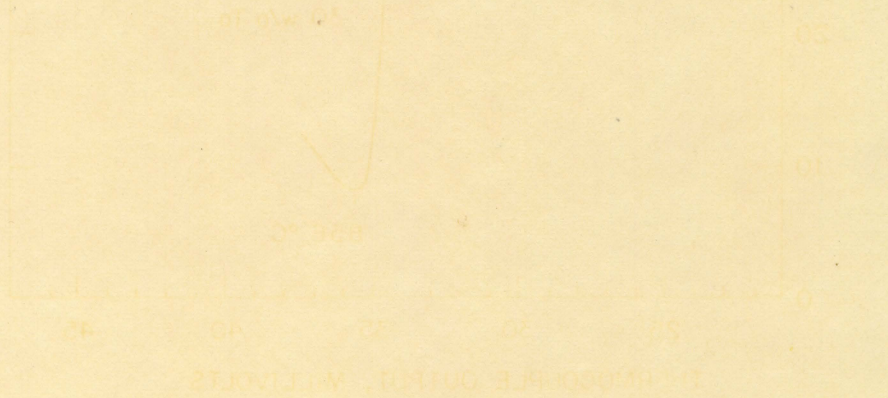


Figure 15. Plots of length vs. temperature obtained on heating for some tantalum-zirconium alloys. The inflections in these curves were caused by the alpha-beta transformation of the zirconium phase. The temperature was measured with a Chromel-Alumel thermocouple.



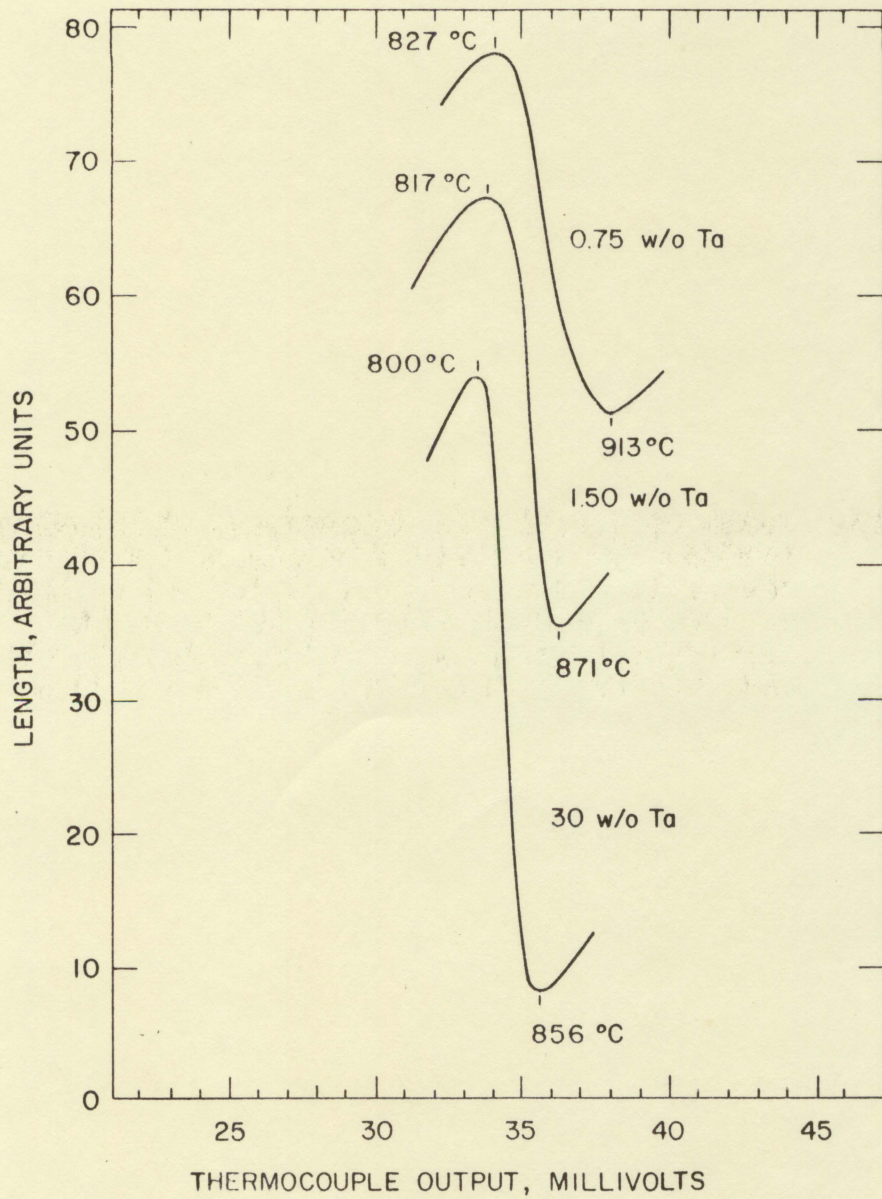


Table 4. Results of temperature-resistance and dilatometric experiments

Composition w/o Ta	Melt number	Inflection on heating, °C ^a	
		Temperature- resistance	Dilatometric
100 w/o Zr	1057	858	860
0.25	1110		860
0.50	1108	840	830
1.75	1109		827
1.00	1106		817
1.50	1124		805
2.00	911	797	
3.00	1037	805	
5.00	1060	795	803
7.00	1061	805	
10.0	1062	798	800
15.0	1063	800	
17.5	1064	800	800
20.0	1065	796	805
25.0	1166		800
30.0	1066	798	798
35.0	1167		805
40.0	1043	803	805
45.0	1071	805	800
50.0	1055	810	807
60.0	1071	805	800
65.0	1121	798	
70.0	1073	810	805
80.0	1087	812	815
90.0	1075	805	807
92.0	1256	820	
94.0	1257	817	
96.0	1258	---b	
98.0	1077	---b	

^aThe values reported are averages of several experiments.

^bNo inflection was observed in the temperature range investigated (room temperature to 1000°C).

Figure 16. 2 w/o tantalum capsule quenched from 915°C, transformed beta structure. 650X.

Figure 17. 1 w/o tantalum capsule quenched from 790°C, alpha solid solution. 650X.

Figure 18. 3 w/o tantalum capsule quenched from 825°C, alpha plus beta. 650X.

Figure 19. 12 w/o tantalum capsule quenched from 805°C, beta solid solution monotectoidally decomposed. 300X.

The photomicrographs illustrate the microstructures observed in alloys quenched from the monotectoid and alpha solid solution regions. All specimens were etched with an ammonium bifluoride-acetic acid-water solution.

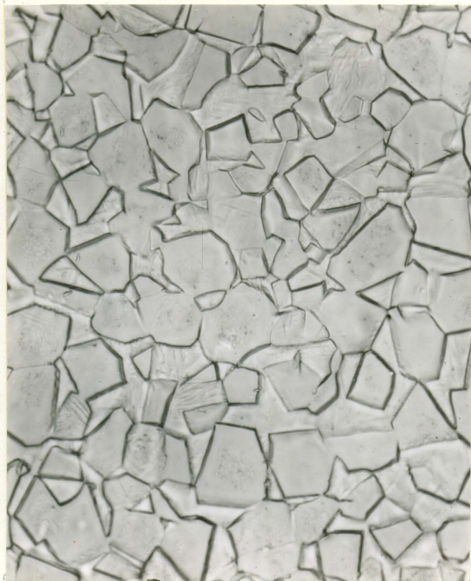
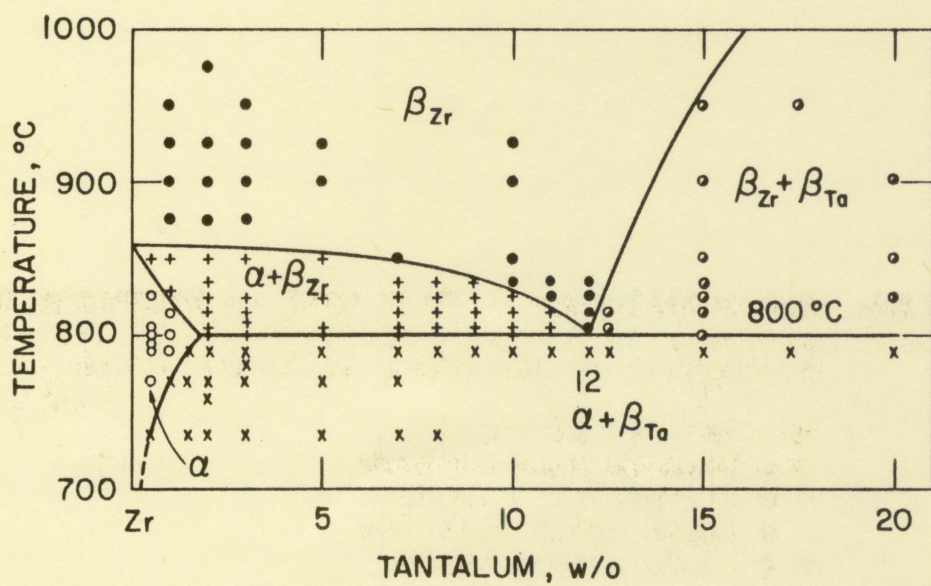




Figure 20. The metallographic data used to determine the location of the monotectoid reaction and the boundaries of the alpha solid solution.

- - Beta solid solution
- ◐ - Beta-Ta plus beta-Zr
- + - Alpha plus beta-Zr
- - Alpha solid solution
- x - Alpha plus beta-Ta



evidence is believed to be less than 0.5 w/o at room temperature. However, the determination of the exact room temperature solubility by metallography was hampered by the presence of nonequilibrium structures and the complicating effect of trace impurities on the interpretation of the microstructures. The low solubility of tantalum at room temperature which was indicated by metallography was supported by X-ray diffraction data. The change in the lattice dimensions of zirconium caused by the solubility of tantalum at room temperature was below the detection limits of the X-ray methods used in this investigation. The calculated value of the lowest solubility limit detectable with the X-ray diffraction methods employed is about 0.5 w/o tantalum.

The metallographic data shown in Figure 13 and the temperature-resistance data contained in Table 4 indicate a solubility of 5 w/o zirconium in tantalum at 800°C. Table 5 contains the lattice parameters of several tantalum-rich alloys which were equilibrated at 1000°C and cooled slowly to room temperature. It can be seen from these data that the lattice parameter of the tantalum-rich phase starts to decrease between 96 w/o and 98 w/o tantalum. Since these alloys almost certainly did not attain room temperature equilibrium, the data show the solubility limit to lie between 96 w/o and 98 w/o tantalum at some temperature above ambient.

Table 5. Lattice parameters of tantalum-rich alloys

Composition w/o Ta	Lattice parameter Å
90	3.3072
92	3.3074
94	3.3070
96	3.3076
98	3.3055
100	3.3035

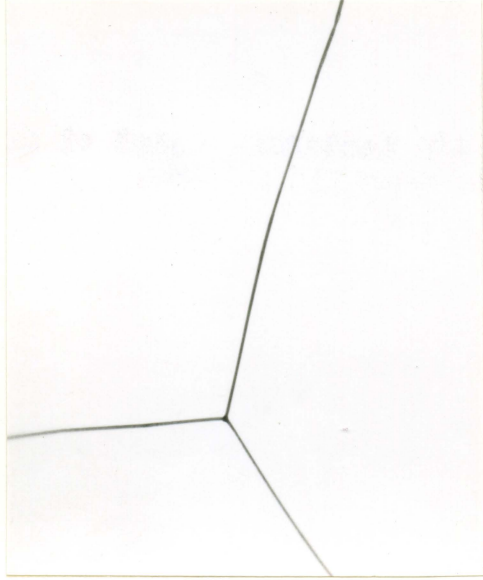
The microstructure shown in Figure 21 is that of the 98 w/o tantalum alloy quenched from 600°C while Figure 22 contains a photomicrograph of the same alloy cooled slowly to room temperature. It is evident that the solubility limit has been slightly exceeded in the latter case.

On the basis of these X-ray and metallographic results it was concluded that the solubility of zirconium in tantalum decreases with temperature from a value of 5 w/o at 800°C to less than 2 w/o at room temperature.

Figure 21. 98 w/o tantalum heated at 600°C for 90 hours then quenched. 250X.

Figure 22. 98 w/o tantalum heated at 1200°C for 120 hours then cooled slowly to room temperature. 250X.

The above specimens were electropolished and etched in a solution of sulphuric and hydrofluoric acids.



SUMMARY

The phase diagram of the tantalum-zirconium alloy system has been presented with an accompanying discussion of the methods used in its investigation.

The solidus of the system exhibits a minimum at 1820°C near 25 w/o tantalum. A complete solid solution of beta zirconium and tantalum exists below the solidus. This solid solution decomposes monotectoidally at 800°C and 12 w/o tantalum. A solid immiscibility loop exists from 12 w/o to 95 w/o tantalum at 800°C and contains a maximum at 80 w/o tantalum and 1780°C. The maximum solubility of tantalum in alpha zirconium is less than 2 w/o and decreases with decreasing temperature. The monotectoid horizontal extends to 95 w/o tantalum where it is terminated by the boundary of the tantalum-rich solid solution. The solubility limit of zirconium in tantalum is less than 2 w/o at room temperature.

ACKNOWLEDGMENTS

The author is grateful to Dr. W. L. Larsen for his interest in the investigation and to Mr. Earl Hopkins for his help in the preparation of the metallographic specimens.

BIBLIOGRAPHY

1. Anderson, C. T., Hayes, E. T., Roberson, A. H., and Kroll, W. J. A preliminary survey of zirconium alloys. U. S. Bureau of Mines Report of Investigations 4658. 1950.
2. Pfeil, P. C. L. A critical review of the alloying behavior of zirconium. United States Atomic Energy Commission Report AERE-M/TN-11 [Ct. Brit. Atomic Energy Research Establishment, Harwell Berks, England]. 1952.
3. Litton, F. B. Ten zirconium alloys evaluated. Iron Age 167, No. 14: 95-99. 1951.
4. Keeler, J. E. Development of zirconium base alloys. General Electric Co. Research Report 56-RL-1648. November, 1956.
5. Chubb, W. Progress in the development of creep resistant zirconium alloys. Trans. Amer. Soc. Metals 48: 804-824. 1956.
6. Van Thyno, R. J. and McPherson, D. J. Elevated temperature strength of selected zirconium base alloys. Trans. Amer. Soc. Metals 48: 795-803. 1956.
7. Emelyanov, V. S., Godin, Yu. G., and Evstyukhin, A. I. Investigation of the system zirconium-tantalum. The Soviet Journal of Atomic Energy 2: 43-49. 1957.
8. Levingston, M. L. and Williams, D. E. Arc melting in the tungsten electrode furnace. U. S. Atomic Energy Commission Report IS-292 [Iowa State Univ. of Science and Technology, Ames. Inst. for Atomic Research]. 1961.
9. Williams, J. T. Vanadium-zirconium alloy system. Trans. Amer. Inst. Min. Met. Engr. 200: 345-350. 1955.
10. Pirani, M. and Alterthum, H. Method for the determination of melting points of metals which fuse at high temperatures. Z. Electrochem. 29: 5-8. 1923.
11. Deoley, M. E. and Atkins, D. F. Electronic vacuum dilatometer. Rev. Sci. Instruments 26: 568-571. 1955.
12. Azaroff, L. V. and Buerger, M. J. The powder method in X-ray crystallography. New York, N. Y., McGraw-Hill Book Co., Inc. 1958.

13. Carlson, A. J., Williams, J. T., Rogers, B. A., and Manthos, E. J. Etching metals by ionic bombardment. U. S. Atomic Energy Commission Report IEC-480 [Ames Lab., Ames, Iowa]. 1954.
14. Lustman, B. and Herze, F. The metallurgy of zirconium. New York, N. Y., McGraw-Hill Book Co., Inc. 1955.
15. Miller, O. L. Tantalum and niobium. New York, N. Y., Academic Press, Inc. 1959.